

PROCEEDINGS OF SPIE

[SPIDigitalLibrary.org/conference-proceedings-of-spie](https://spiedigitallibrary.org/conference-proceedings-of-spie)

Computation of the optical properties of tissues from light reflectance using a neural network

Lihong V. Wang, Xuemei Zhao, Steven L. Jacques

Lihong V. Wang, Xuemei Zhao, Steven L. Jacques, "Computation of the optical properties of tissues from light reflectance using a neural network," Proc. SPIE 2134, Laser-Tissue Interaction V; and Ultraviolet Radiation Hazards, (17 August 1994); doi: 10.1117/12.182973

SPIE.

Event: OE/LASE '94, 1994, Los Angeles, CA, United States

Computation of the optical properties of tissues from light reflectance using a neural network

Lihong Wang, Xuemei Zhao, and Steven L. Jacques
Laser Biology Research Laboratory, Box 17
The University of Texas M. D. Anderson Cancer Center
1515 Holcombe Boulevard, Houston, Texas 77030

ABSTRACT

We have established a neural network to quickly deduce optical properties of tissue slabs from the diffuse reflectance distribution. Diffusion theory based on multiple image sources mirrored about the two extrapolated boundaries is used to prepare the training and testing sets for the neural network. The neural network is trained using backpropagation with the conjugate gradient method. Once the neural network is trained, it is able to deduce optical properties of tissues within on the order of a millisecond. The range of the tissue optical properties that is covered by our neural network is $0.01\text{-}2\text{ cm}^{-1}$ for absorption coefficient, $5\text{-}25\text{ cm}^{-1}$ for reduced scattering coefficient, and $0.001\text{-}1\text{ cm}$ for tissue thickness. A separate network is also trained for thick tissue slabs. A simple experimental setup applying the trained neural network is designed to measure tissue optical properties quickly.

INTRODUCTION

When lasers are used for diagnosis or for therapy of disease, it is important to know the tissue optical properties. The many traditional methods of measuring these optical properties use integrating spheres,^{1,2} optical-fiber bundles,³ charge-coupled device (CCD) cameras,⁴ time-resolved reflectance,⁵⁻⁷ photon-density waves,^{8,9} and photo-acoustic waves.¹⁰ Each method has both advantages and disadvantages.

The method of using integrating spheres,^{1,2} considered the gold standard for in vitro measurement, gives reasonably reliable results when it is carefully performed. The most common source of error results from the lateral loss of light through the tissue slab sandwiched with two glass slides and from the light bouncing from the sphere wall back into the tissue. The lateral loss is determined by the port size of the integrating sphere and the optical properties of the tissue. The inverse problem of finding the optical properties of the tissue from the measurement is very slow and/or complicated. When the fast adding-doubling method is used to solve the inverse problem, correction factors have to be used to account for the light loss. When the slow Monte Carlo method is used to solve the inverse problem, hours of work are required.

The traditional methods of using optical-fiber bundles³ and CCD cameras⁴ measure the spatial distribution of diffuse reflectance. Then, nonlinear least-squares fit is used to extract the optical properties of tissues based on the diffusion theory for infinitely thick tissue slabs. The diffusion theory is much faster than Monte Carlo simulations but is limited to simple geometries.

Time-resolved diffuse reflectance⁵⁻⁷ can be used to accurately measure the absorption coefficient of a semi-infinite medium because the tail of the signal after a sufficiently long time relies primarily on the absorption coefficient. This method can even be used to measure the optical properties of a thick tissue layer underlying a thin tissue layer. The diffuse reflectance will depend more on the bottom layer than on the upper layer as time elapses,¹¹ and the slope of the tail of the diffuse reflectance is primarily determined by the optical properties of the bottom layer. However, this approach requires expensive ultrashort lasers (<1 picosecond pulse width) and fast detectors. The equivalent of the time-resolved approach in the frequency domain, photon-density wave

measurements,^{8,9} is a cheaper alternative. This technique is currently limited to semi-infinite media.

Photo-acoustic waves¹⁰ can be used to measure the effective attenuation coefficient of a semi-infinite tissue very easily and to measure the thickness of each layer in multilayered tissues. Instead of measuring the light escaping from the tissue, this technique measures the light-induced acoustic waves emitted from inside the tissue and may have the potential for use in tissue imaging. However, the inverse algorithm to deduce the tissue optical properties can be complicated.

The neural network approach of measuring optical properties of tissue has been recently introduced by Farrell et al.¹² They have established a neural network to deduce the optical properties of semi-infinite tissues. Kienle et al¹³ and our group have independently and simultaneously presented a neural network approach for tissue slabs. They measure the light transmittance through a tissue slab that has a fixed thickness and then deduce the absorption coefficient and the reduced scattering coefficient of the tissue slab. We measure the diffuse reflectance from a tissue slab with a variable thickness between 10 μm and 1 cm and deduce the optical properties of the tissue from the diffuse reflectance. A simple experimental setup is subsequently presented in this paper. The most salient feature of the neural network approach is that once the network is trained, it can deduce the optical properties of tissues in real time (on the order of a millisecond).

METHODS

A neural network is used to deduce the optical properties of a tissue slab from the spatially resolved diffuse reflectance. The neural network requires training with examples, which are pairs of diffuse reflectance and the corresponding optical properties. Monte Carlo simulations would be the ideal tool to prepare the example set if it were faster. We use the diffusion theory to prepare the example set, being careful to avoid the region where the diffusion theory fails.

The optical properties that we want to measure are the absorption coefficient (μ_a) and the reduced scattering coefficient (μ_s'). Two related coefficients are the transport interaction coefficient (μ_t') and the effective attenuation coefficient (μ_{eff}), which are respectively expressed by the following relationship:

$$\mu_t' = \mu_a + \mu_s' \quad (1)$$

and

$$\mu_{\text{eff}} = \sqrt{3 \mu_a \mu_t'} \quad (2)$$

The inverse of the transport interaction coefficient is defined as one transport mean free path ($\text{mfp}' = 1/\mu_t'$).

DIFFUSION THEORY

Diffusion theories for semi-infinite tissues have been presented elsewhere.¹⁴ In this paper, we extend the diffusion theory for tissue slabs. An infinitely narrow laser beam (pencil beam) is incident upon a tissue slab whose optical properties are refractive index n , μ_a , μ_s' , and thickness d . The pencil beam is approximated by an isotropic point source that is 1 mfp' below the tissue surface.

A cylindrical coordinate system is set up, where the z axis originates on the top tissue surface and points downward perpendicularly to the tissue surface. In this cylindrical coordinate system, the fluence caused by an isotropic point source at $z = z_s$ in an otherwise infinite medium has been analytically solved, i.e.,

$$\phi(z, r, z_s) = \frac{1}{4 \pi D} \frac{\exp(-\mu_{\text{eff}} \rho)}{\rho}, \quad (3)$$

where z and r are the cylindrical coordinates of the observation point and ρ is the distance between the observation point and the source, i.e.,

$$\rho = \sqrt{(z - z_s)^2 + r^2}, \quad (4)$$

and D is the diffusion constant,

$$D = 1/(3 \mu_t'). \quad (5)$$

Since we are interested in the reflectance on the top tissue surface, the contribution of this isotropic point source is

$$J(z=0, r, z_s) = D \left. \frac{\partial \phi}{\partial z} \right|_{z=0} = \frac{z_s (1 + \mu_{\text{eff}} \rho) \exp(-\mu_{\text{eff}} \rho)}{4 \pi \rho^3}. \quad (6)$$

The transmittance on the bottom tissue surface can be computed similarly.

To compute the fluence caused by an isotropic point source in a tissue slab based on Eq. (3), we need to convert the slab into an infinite medium by satisfying the boundary condition with an array of image sources. Since the fluence on the two real boundaries is not zero, two extrapolated virtual boundaries where the fluence is approximately zero are used. The two virtual boundaries are the distance z_b away from the tissue surfaces, where z_b is

$$z_b = 2 A D, \quad (7)$$

where A is related to the internal reflection r_i . When the boundary has matched refractive indices, $A = 1$; otherwise, A can be estimated by

$$A = (1 + r_i)/(1 - r_i), \quad (8)$$

where

$$r_i = -1.440 n_{\text{rel}}^{-2} + 0.710 n_{\text{rel}}^{-1} + 0.668 + 0.0636 n_{\text{rel}}, \quad (9)$$

where n_{rel} is the relative refractive index of the tissue.¹⁵

Fig. 1 shows the positions of the original isotropic point source and its image sources about the two virtual boundaries. Each mirroring changes the sign of the point source. The z coordinate of its positive or negative image source is

$$z_i(\pm) = -z_b + i (d + 2z_b) \pm (z_0 + z_b). \quad (10)$$

Once these image sources are used, the boundary condition is approximately satisfied, and hence the true boundaries can be removed. The problem is converted into an array of isotropic sources of both signs in an infinite medium. A linear combination of Eq. (3) for different source positions will, therefore, yield the fluence of the isotropic point source in the original tissue slab, and a linear combination of Eq. (6) for different source positions will yield the reflectance.

Results of our method computing the diffuse reflectance and transmittance are compared with those computed by the Monte Carlo method¹⁶ in Fig. 2, in which the Monte Carlo simulation results are considered accurate. Although the number of image sources is infinite, the series is truncated after four pairs of sources. For the diffuse reflectance, the diffusion theory is accurate only after r is beyond a couple of mfp' . For the diffuse transmittance, the diffusion theory seems to be accurate even for small r values, but the Monte Carlo simulation result is too noisy to permit a definitive conclusion.

More photons will be traced to investigate this matter.

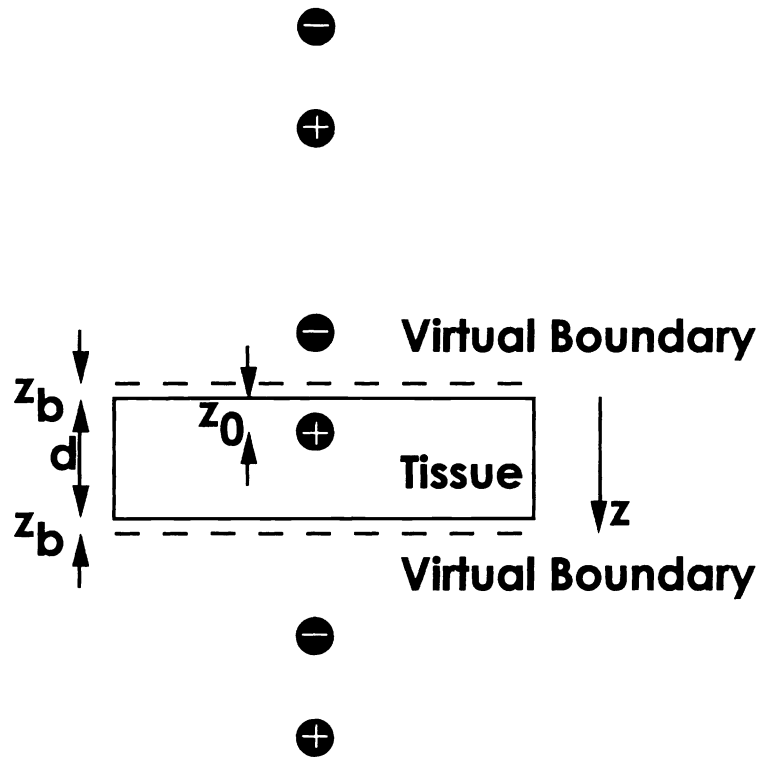


Fig. 1. Distribution of the image sources for a tissue slab. The original isotropic point source is $z_0 = 1 \text{ mfp}'$ below the tissue surface.

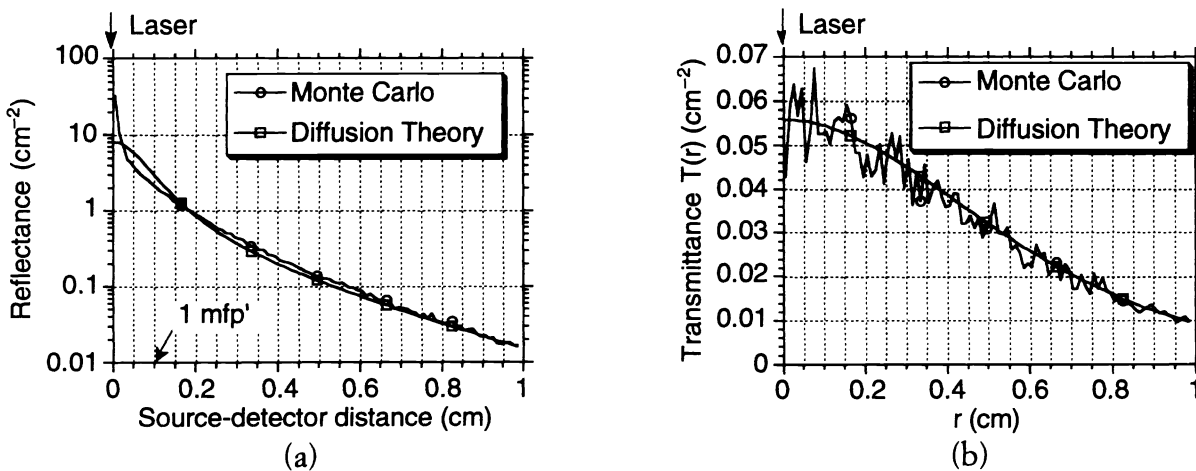


Fig. 2. (a) Diffuse reflectance and (b) diffuse transmittance of a pencil beam incident upon a tissue slab are computed with the diffusion theory and compared with the Monte Carlo simulation. The slab thickness is 1 cm, and the optical properties of the tissue are refractive index $n_{\text{rel}} = 1.37$, $\mu_a = 0.1 \text{ cm}^{-1}$, and $\mu_s' = 10 \text{ cm}^{-1}$.

Various optical properties and tissue thicknesses have been used to compute the diffuse

reflectance and transmittance. We have found that the following conditions must be satisfied to assure the accuracy of the diffusion theory for tissue slabs:

$$\mu_a \ll \mu_s' \quad (11)$$

and

$$d \geq 4 \text{ mfp}' \quad (12)$$

NEURAL NETWORK

A neural network is essentially a nonlinear matrix operator that converts the input to the output. In our particular application, the input is the diffuse reflectance as a function of r , and the output is the optical properties of tissues. The optical properties that we want to measure are μ_a and μ_s' . It is noticed that the slope of $\ln[R(r) r^2]$ vs. r for a semi-infinite medium is approximately $-\mu_{\text{eff}}$ when r is sufficiently large.¹² Therefore, it is advantageous to use $\ln[R(r) r^2]$ at different r positions as the input to the neural network and μ_{eff} as one of the outputs.

Because the diffuse reflectance $R(r)$ computed with the diffusion theory becomes valid only for $r \geq \text{mfp}'$, the data at $r < \text{mfp}'$ will not be used and we choose an r range from r_{min} to r_{max} for the input of the neural network. Because we will measure only the relative values of $R(r)$ in the experiment, we normalize $R(r)$ by $R(r_{\text{min}})$. Therefore, the input to the neural network is $\ln[r^2 R(r)/R(r_{\text{min}})]$. The two outputs of the neural network are chosen to be μ_{eff} and μ_t' (Fig. 3).

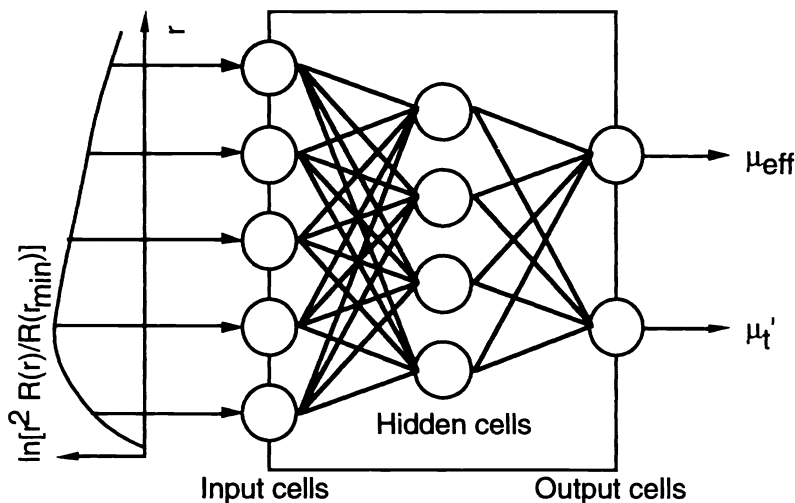


Fig. 3. Illustration of the neural network. In this example, five input cells, four hidden cells, and two output cells are used. The input to the neural network is $\ln[r^2 R(r)/R(r_{\text{min}})]$ at five different radial positions. The output is μ_{eff} and μ_t' .

A range of optical properties and tissue thicknesses are chosen for the neural network. Diffuse reflectances for different optical properties and slab thickness are computed at given radial positions with the diffusion theory. They are prepared in the format that the neural network accepts and are then used as the training examples. The two optical properties for the outputs of the neural network are scaled to fit in the range 0.1 to 1. A public domain program is used to train the neural network.¹⁷ The backpropagation with the conjugate gradient algorithm is selected to minimize the error.

RESULTS

We have established a neural network to deduce optical properties of tissue slabs. The optical properties of the tissues are refractive index $n_{\text{rel}} = 1.37$, $\mu_a = 0.01\text{-}2 \text{ cm}^{-1}$, and $\mu_s' = 5\text{-}25 \text{ cm}^{-1}$, and

the thicknesses are $d = 0.001-1$ cm. The radial positions are 9 points evenly distributed between $r = 0.2-1.5$ cm. The neural network has 9 input cells, 10 hidden cells, and 2 output cells. The tissue thickness is not used as input information to the neural network, and the neural network is able to deduce the optical properties without this information. This feature makes the experiment of measuring optical properties very convenient.

After the neural network is trained, it is tested with multiple pairs of diffuse reflectance and the corresponding known optical properties. When the diffuse reflectance is fed into the neural network, the output values of the neural network are compared with the known exact optical properties to evaluate the error of the neural network (Fig. 4). If the neural network output values are exactly the same as the exact values, then all data points in the figure should be on the diagonal line. Data points offset from the diagonal line indicates a discrepancy between the neural network output values and the correct values. Most data points are within the $\pm 10\%$ error zone with respect to the expected output values of the neural network except for those points in the low μ_{eff} region (circled in Fig. 4a). Both the rms error of μ_{eff} outside of the ellipse in Fig. 4a and the rms error of the μ_t' are less than 5%. Based on the speed of the testing on a Sun SPARCstation 10 computer, it is estimated that the neural network is able to deduce the optical properties of tissues within on the order of a millisecond.

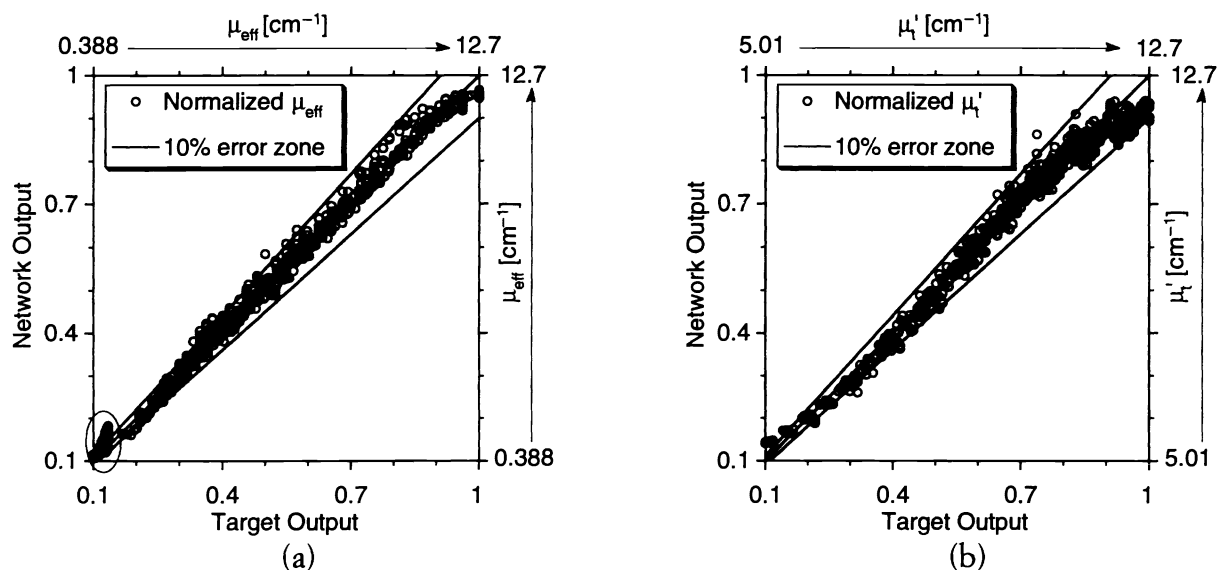


Fig. 4. The testing results of the neural network for tissue slabs, in which the target output is the known exact optical properties and the network output is from the network when the diffuse reflectance is fed into the neural network.

We have also set up a neural network to deduce optical properties of semi-infinite tissues. The optical properties of the tissues are refractive index $n_{\text{rel}} = 1.37$, $\mu_a = 0.005-2.5$ cm^{-1} , and $\mu_s' = 5-20$ cm^{-1} . The input to the neural network is $\ln[r^2 R(r)/R(0)]$ at 8 radial positions that are evenly distributed between $r = 0.1-2$ cm. The neural network has eight input cells, nine hidden cells, and two output cells. The testing results are shown in Fig. 5. Most data points are within the $\pm 10\%$ error zone except for those in the circles that have low μ_{eff} and μ_t' . The rms error for both the outputs of the neural network excluding the circled regions is 3%. Note that the output values of this neural network are scaled to the range of 0-1 instead of 0.1-1.

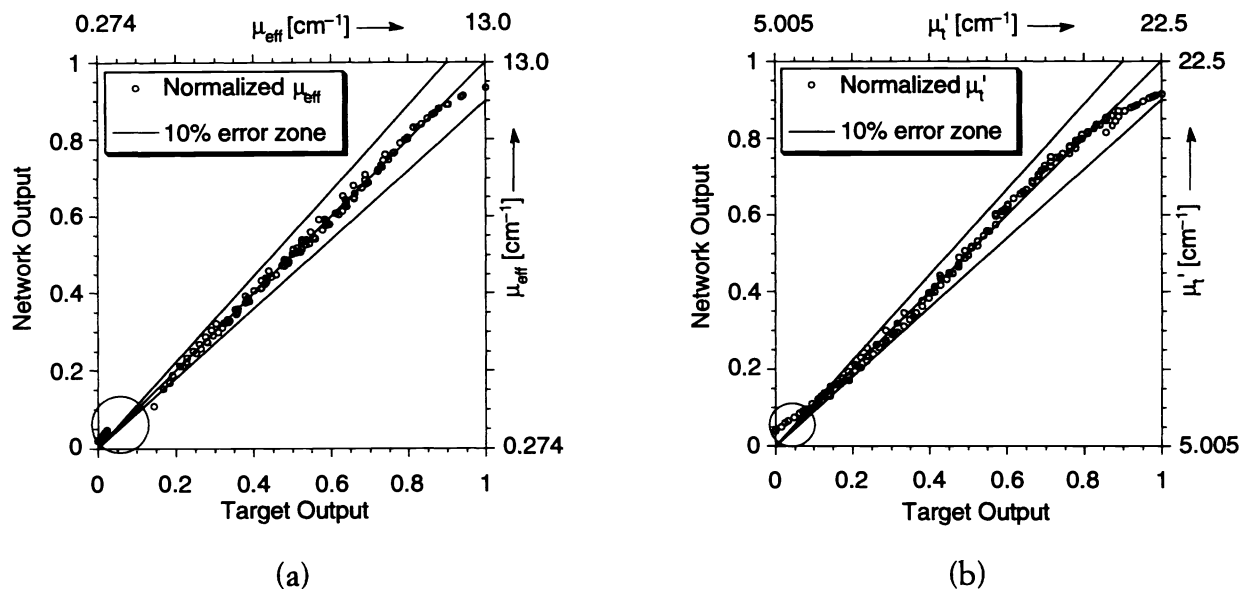


Fig. 5. The testing results of the neural network for semi-infinite tissues.

DISCUSSION

The neural network has proven to be a very quick and simple approach to measuring optical properties of tissues. All we need from the experiment is the diffuse reflectance as a function of the radial position. A simple CCD camera-based experimental setup modified from our previous version⁴ is shown in Fig. 6. A tissue sample is laid on top of an absorbing base. A collimated laser beam is directed onto the top tissue surface. The diffuse reflectance pattern is collected by the CCD camera and transferred to a computer. The computer prepares the diffuse reflectance in the correct format for the trained neural network, and the neural network yields the effective attenuation coefficient μ_{eff} and the transport interaction coefficient μ_t' . The computer then converts μ_{eff} and μ_t' into μ_a and μ_s' .

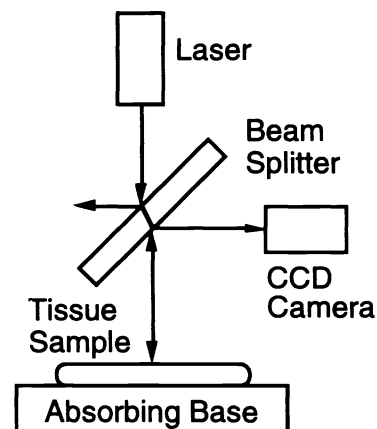


Fig. 6. The experimental setup (not drawn to scale) to be used to measure the diffuse reflectance as a function of the radial position. The beam splitter is used to align the optical axes of the laser beam and the CCD camera.

The reason we use an absorbing base to support the tissue slab is to absorb all the transmitted light, otherwise the transmitted light that is reflected back into the tissue slab will complicate the computation of optical properties. Because the neural network does not require the use of tissue thickness as input, it is not necessary measure the thickness of the tissue slab provided that the tissue thickness is within the range of specification of the neural network. For the neural network presented here, the thickness has to be between 10 μm and 1 cm.

Once the setup is aligned, only one line of pixels on the CCD camera need to be quickly transferred to the computer. It takes the computer on the order of only one millisecond to deduce the

optical properties of tissues using the neural network. Therefore, the setup can measure optical properties of tissues in real time. A plug-in hardware card can be added to the computer to implement the neural network to further enhance the speed.

The application of this setup is potentially diverse. Besides measuring optical properties of tissues in slab geometry, it can be extended to measure optical properties of semi-infinite tissues by replacing the neural network. Heating the tissue samples will allow measurement of the optical properties as a function of temperature, the optical properties of the heated tissues are believed to be important data for photo-thermal applications of lasers.

In summary, we believe the neural network approach will provide a quick and simple tool for measuring the optical properties of tissues.

ACKNOWLEDGMENTS

We thank Linda Eppich for proofreading the manuscript. This research was supported in part by the Office of Naval Research (N00014-91-J-1354), the Air Force Office of Scientific Research (F49620-93-1-0298DEF), and the National Institutes of Health (R29-HL45045).

REFERENCES

1. J. W. Pickering, S. A. Prahl, N. Vanwieringen, J. F. Beek, H. J. C. M. Sterenborg, and M. J. C. Vangemert, "Double-integrating-sphere system for measuring the optical-properties of tissue," *Applied Optics*, 32 (4), 399-410 (1993).
2. M. Firbank, M. Hiraoka, M. Essenpreis, and D. T. Delpy, "Measurement of the optical properties of the skull in the wavelength range 650-950 nm," *Phys. Med. Biol.*, 38, 503-510 (1993).
3. B. C. Wilson, T. J. Farrell, and M. S. Patterson, "An optical fiber-based diffuse reflectance spectrometer for non-invasive investigation of photodynamic sensitizers in vivo," *Proc. SPIE*, 6, 219-232 (1990).
4. S. L. Jacques, A. Gutsche, J. A. Schwartz, L.-H. Wang, F. K. Tittel, "Video reflectometry to extract optical properties of tissue in vivo," *Proc. SPIE*, 11, 211-226 (1993).
5. M. S. Patterson, B. Chance, B. C. Wilson, "Time resolved reflectance and transmittance for the non-invasive measurement of tissue optical properties," *Applied Optics*, 28, 2331-2336 (1989).
6. S. L. Jacques, L.-H. Wang, A. H. Hielscher, "Time-resolved photon propagation in tissues," In: A. J. Welch, M. J. C. van Gemert (ed.), *Optical Thermal Response of Laser Irradiated Tissue*, in press; Plenum Publishing Corp., New York, 1994.
7. H. Liu, M. Miwa, B. Beauvoit, N. G. Wang, B. Chance, "Characterization of absorption and scattering properties of small-volume biological samples using time-resolved spectroscopy," *Anal. Biochem.*, 213 (2), 378-385 (1993).
8. M. S. Patterson, J. D. Moulton, B. C. Wilson, K. W. Berndt, J. R. Lakowicz, "Frequency domain reflectance for the determination of the scattering and absorption properties of tissue," *Applied Optics*, 30, 4474-4476 (1991).
9. B. J. Tromberg, L. O. Svaasand, T. T. Tsay, R. C. Haskell, "Properties of photon density waves in multiple-scattering media," *Applied Optics*, 32 (4), 607-616 (1993).
10. S. L. Thomsen, H. Vijverberg, S. L. Jacques, A. A. Oraevsky, "Optical properties of albino rat skin heated in vitro: comparison of photoacoustic and integrating sphere measurement techniques," *Proc. SPIE*, 2134A, in press (1994).
11. A. H. Hielscher, H. Liu, F. K. Tittel, B. Chance, L.-H. Wang, S. L. Jacques, "Determination of blood oxygenation in the brain by time-resolved reflectance spectroscopy I," *Proc. SPIE*, 2136A, in press (1994).

12. T. J. Farrell, B. C. Wilson, and M. S. Patterson, "The use of a neural network to determine tissue optical properties from spatially resolved diffuse reflectance measurements," *Phys. Med. Biol.*, 37 (12), 2281-2286 (1992).
13. A. Kienle, R. Hibst, R. W. Steiner, "Use of a neural network and Monte Carlo simulations to determine the optical coefficients with spatially resolved transmittance measurements," *Proc. SPIE*, 2134A, in press (1994).
14. T. J. Farrell, M. S. Patterson, and B. C. Wilson, "A diffusion theory model of spatially resolved, steady-state diffuse reflectance for the non-invasive determination of tissue optical properties in vivo," *Med. Phys.*, 19 (4), 879-888 (1992).
15. R. A. J. Groenhuis, H. A. Ferwerda, and J. J. Ten Bosch, "Scattering and absorption of turbid materials determined from reflection measurements. I: Theory," *Applied Optics*, 22 (16), 2456-2462 (1983).
16. L.-H. Wang and S. L. Jacques, "Monte Carlo modeling of light transport in multi-layered tissues in standard C," The University of Texas M. D. Anderson Cancer Center, Houston, Texas, 1992.
17. D. van Camp, "A users guide for the Xerion neural network simulator," Department of Computer Science, University of Toronto, 1993.

